

## POWER FLATTENING AND REACTIVITY SUPPRESSION STRATEGIES FOR THE CANADIAN SUPERCRITICAL WATER REACTOR CONCEPT

**M. McDonald, A. Colton, J. Pencer**

Canadian Nuclear Laboratories, Chalk River, Ontario, Canada  
[michael.mcdonald@cnl.ca](mailto:michael.mcdonald@cnl.ca)

### **Abstract**

The Canadian supercritical water-cooled reactor (SCWR) is a conceptual heavy water moderated, supercritical light water cooled pressure tube reactor. In contrast to current heavy water power reactors, the Canadian SCWR will be a batch fuelled reactor. Associated with batch fuelling is a large beginning-of-cycle excess reactivity. Furthermore, radial power peaking arising as a consequence of batch refuelling must be mitigated in some way. In this paper, burnable neutron absorber (BNA) added to fuel and absorbing rods inserted into the core are considered for reactivity management and power flattening. A combination of approaches appears adequate to reduce the core radial power peaking, while also providing reactivity suppression.

### **1. Introduction**

The Canadian supercritical water-cooled reactor (SCWR) is an advanced, Generation-IV reactor concept being developed by Canadian Nuclear Laboratories (CNL) with national and international collaborators through the support of Natural Resources Canada (NRCAN) [1]. The concept is a pressure tube-based, heavy water moderated, light water cooled reactor. Key features of the concept include enhanced safety, to be achieved through the use of the moderator to remove long term decay heat under various postulated accidents, and enhanced thermal efficiency, to be achieved through the use of supercritical water coolant in tandem with a direct thermodynamic cycle [2].

Previous reactor physics investigations have presented results on key SCWR physics parameters such as: exit burnup, channel peaking factors, coolant void reactivity ([3], [4]) and most recently, core kinetics parameters [5]. All previous studies have investigated so-called device-free cores, i.e. no reactivity control devices have been modelled for suppression of reactivity and power shaping. The current work incorporates control rods, analogous to the adjuster rods in a heavy water reactor (HWR), which remain in the core during normal operation for reactivity suppression. A further refinement to the SCWR concept, burnable neutron absorber (BNA) has been introduced into the fuel assembly to provide further initial reactivity suppression. The results of core calculations with these changes to the concept are presented in this paper.

### **2. Lattice and Core Descriptions**

#### **2.1 Lattice Description**

The current Canadian SCWR concept features a core with 336 vertical fuel channels, with each channel containing a 5 metre long fuel assembly. The fuel channel is made up of a pressure tube in direct contact with the surrounding moderator. On the inside of the pressure tube is a zirconia insulator and a

zirconium-modified stainless steel liner tube. The fuel assembly itself is made up of two rings of 32 plutonia-thoria fuel elements. One significant modification from previous versions of the SCWR lattice is the addition of BNA to eight of the elements in each of the rings. These elements contain 4% gadolinia ( $Gd_2O_3$  in  $PuO_2/ThO_2$ ) to provide initial reactivity suppression in fresh fuel. The gadolinia-containing elements have been staggered mainly to reduce temperature effects. The rationale behind this choice of burnable neutron absorber is discussed in the results section of this paper. The lattice cell is illustrated in Figure 1, while material and geometry specifications are listed in Table 1.

The centre portion of the fuel channel contains a coolant flow tube. Coolant enters from the top of the core, flows down through the flow tube, reverses direction at the end of the channel, and flows back up over the fuel, and exits the reactor through outlets above the channels. The presence of a large volume of water in the centre of the fuel assembly provides a substantial amount of neutron moderation. This moderation leads to balanced power profiles in the two rings of fuel, as well as a negative coolant void coefficient. A cross-sectional view of the SCWR, with schematic illustrating the flow tube, is shown in Figure 2.

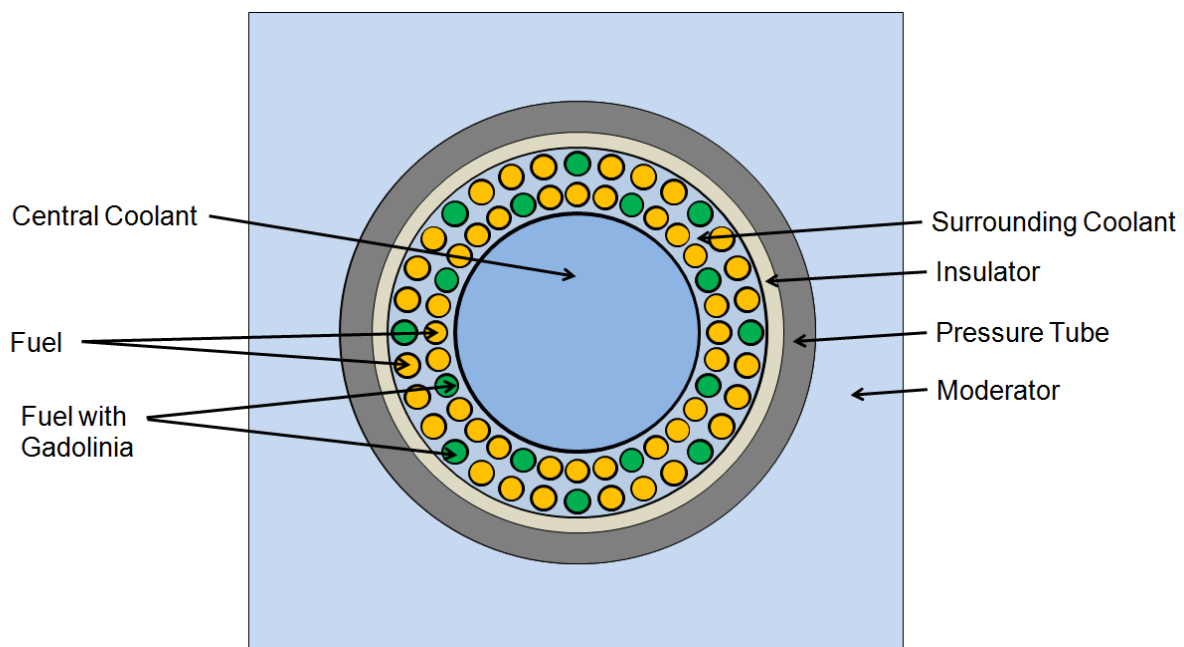


**Figure 1** Cross-sectional view of the 64-element SCWR assembly, channel, and lattice cell

**Table 1 Material and Geometry Specifications**

| Component                          | Dimension   | Material   | Composition (wt%)   | Density (g/cm <sup>3</sup> ) |
|------------------------------------|---|--|---|------------------------------|
| Central Coolant (inside flow tube) | 4.60 cm radius  | Light Water  | 100% H <sub>2</sub> O   | variable                     |
| Flow Tube Inner Cladding           | 4.60 cm inner radius (IR)<br>0.1 cm thick   | Zr-modified 310 Stainless Steel (Zr-mod SS)  | C:0.034; Si:0.51; Mn:0.74; P:0.016; S:0.0020; Ni:20.82; Cr:25.04; Fe:51.738; Mo:0.51; Zr:0.59 | 7.90                         |
| Inner Pins (No BNA) (24)           | 0.415 cm radius<br>5.4 cm pitch circle radius   | 15 wt% PuO <sub>2</sub> /ThO <sub>2</sub>  | Pu:13.23; Th:74.70; O:12.07   | 9.91                         |
| Outer Pins (No BNA) (24)           | 0.440 cm radius<br>6.575 cm pitch circle radius                                       | 12 wt% PuO <sub>2</sub> /ThO <sub>2</sub>  | Pu:10.59; Th:77.34; O:12.08   | 9.87                         |
| Inner Pins (BNA) (8)               | 0.415 cm radius<br>5.4 cm pitch circle radius (evenly spaced, $\pi/8$ angular offset) | 15 wt% PuO <sub>2</sub> /ThO <sub>2</sub> ; 4 wt% Gd <sub>2</sub> O <sub>3</sub> in PuO <sub>2</sub> /ThO <sub>2</sub> | Pu: 12.70; Th: 71.71; Gd 3.47; O: 12.52   | 9.80                         |
| Outer Pins (BNA) (8)               | 0.440 cm radius<br>6.575 cm pitch circle radius (evenly spaced, no angular offset)    | 12 wt% PuO <sub>2</sub> /ThO <sub>2</sub> ; 4 wt% Gd <sub>2</sub> O <sub>3</sub> in PuO <sub>2</sub> /ThO <sub>2</sub> | Pu: 10.16; Th: 74.24; Gd 3.47; O: 12.12   | 9.76                         |
| Cladding                           | 0.06 cm thick   | Zr-mod SS  | As above  | 7.90                         |
| Coolant                            | n/a   | Light Water  | 100% H <sub>2</sub> O   | variable                     |
| Liner Tube                         | 7.20 cm IR<br>0.05 cm thick   | Zr-mod SS  | As above  | 7.90                         |
| Insulator                          | 7.25 cm IR<br>0.55 cm thick   | Zirconia (ZrO <sub>2</sub> )   | Zr:66.63; Y:7.87; O:25.5  | 5.83                         |
| Outer Liner                        | 7.80 cm IR<br>0.05 cm thick   | Excel (Zirconium Alloy)  | Sn:3.5; Mo:0.8; Nb:0.8; Zr:94.9   | 6.52                         |
| Pressure Tube                      | 7.85 cm IR<br>1.2 cm thick  | Excel (Zirconium Alloy)  | Sn:3.5; Mo:0.8; Nb:0.8; Zr:94.9   | 6.52                         |
| Moderator                          | 25 cm square lattice pitch  | D <sub>2</sub> O   | 99.833 D <sub>2</sub> O; 0.167 H <sub>2</sub> O   | variable (1.0851, nominal)   |
|                                    |   | Reactor Grade-Pu   | Pu-238:2.75; Pu-239:51.96; Pu-240:22.96; Pu-241:15.23; Pu-242:7.10                            |                              |
| Adjuster Rods                      | 3.3 cm radius   | Stainless steel alloy 304L   | C: 0.037; Fe: 72.761; Si: 0.46; Ni: 8.43; Mn: 1.282; Cr: 17.12                                | 7.9                          |

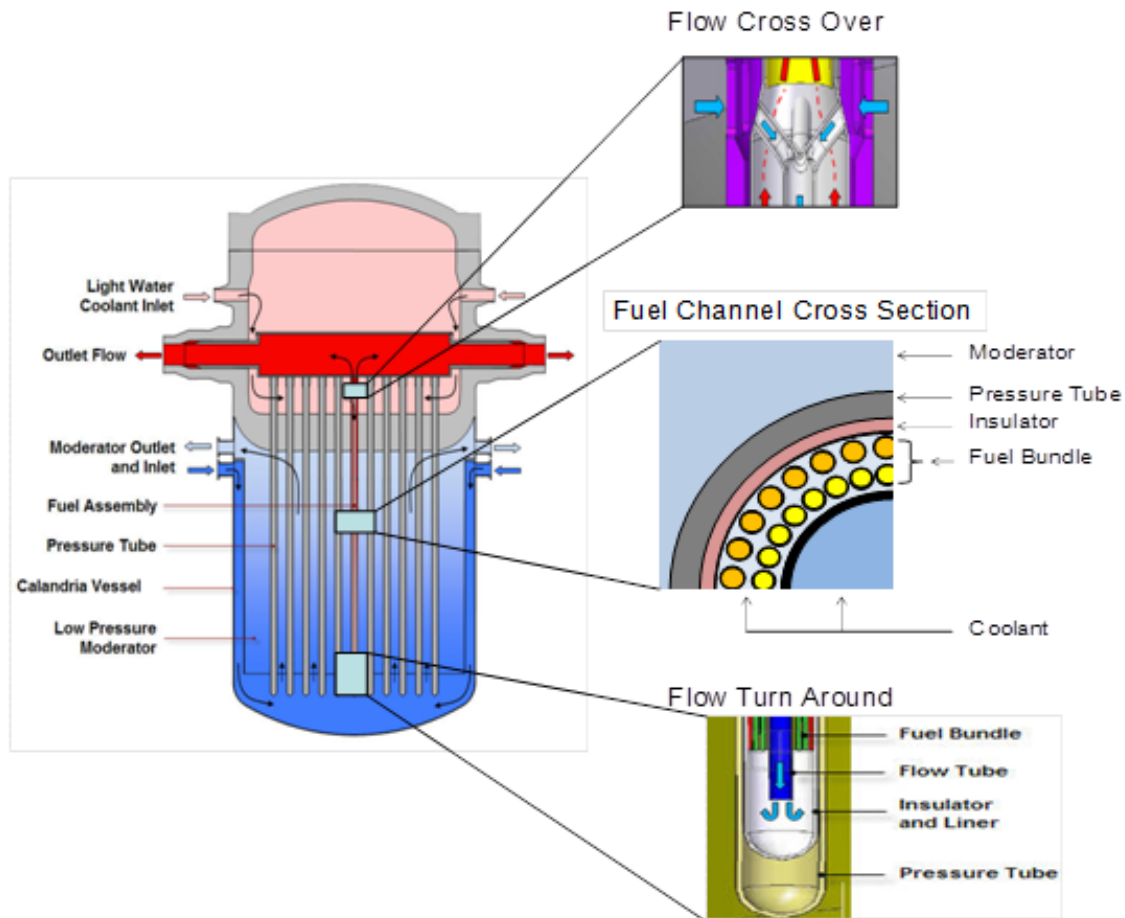


Figure 2 SCWR Core Schematic (from [6])

## 2.2 Core Description

The SCWR is intended to generate 2540 MW of thermal power. Nominal core parameters are listed in Table 2. The three-batch refuelling scheme (shown in Figure 3) remains unchanged from previous studies. Improvements in the channel power distribution and axial power peaking factors may be possible through further adjustments of the refuelling scheme but were not investigated in this study.

The adjuster rods used in this study are modelled after stainless steel CANDU adjuster rods. The rods are cylindrical with a radius of 3.3 cm, composed of stainless steel alloy 304L with composition provided in Table 1. Further information about rods and their locations is provided in Section 4.2.1.

Table 2 Nominal Core Specifications

| Parameter                   | Value           |
|-----------------------------|-----------------|
| Thermal Power               | 2540 MW         |
| Electric Power              | 1200 MW         |
| Inlet / Outlet temperatures | 350°C / 625°C   |
| Inlet / Outlet pressures    | 26 MPa / 25 MPa |
| Channels                    | 336             |

|  |   |
|--|---|
| Lattice Pitch  | 25 cm                                     |
| Core Radius (including radial reflector region)                  | 355 cm                                    |
| Core Height (including axial D <sub>2</sub> O reflector regions) | 650 cm                                    |
| Upper axial reflector thickness                                  | 75 cm                                     |
| Lower axial reflector thickness                                  | 75 cm                                     |
| Fuel Assembly Length   | 500 cm                                    |
| Fuel batches   | 3   |
| Target exit burnup   | 40 MWd / kg                               |
| Target CVR   | < 0                                       |
| Adjuster Rods  | Five vertical banks of 14 horizontal rods |

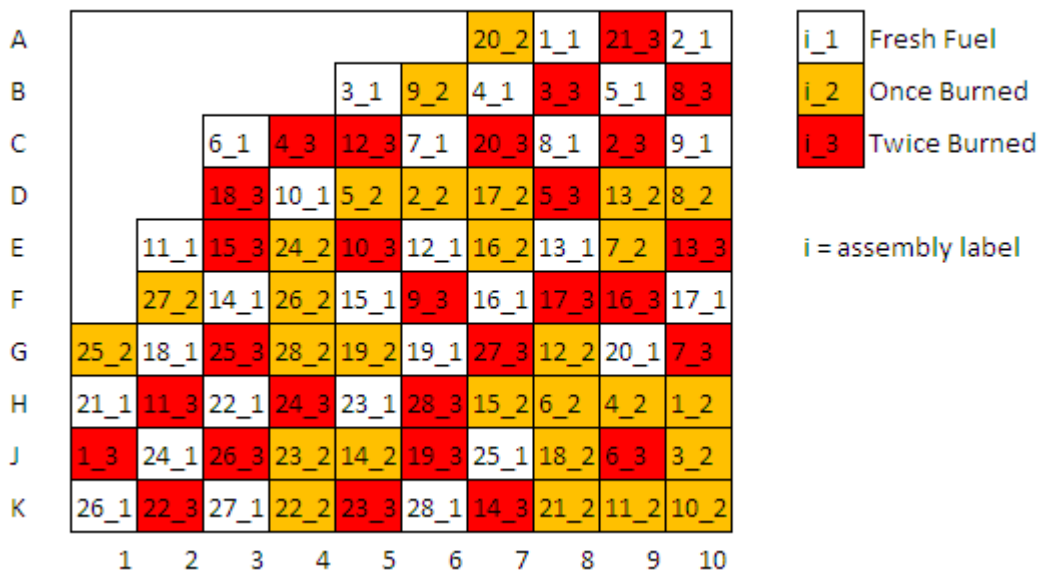


Figure 3 SCWR quarter core channel map and fuel loading scheme

### 3. Codes Used

Lattice physics calculations were performed using WIMS-AECL 3.1.2 [7] with an ENDF/B VII.0 based nuclear data library [8]. Two group homogenized cross sections were produced from WIMS-AECL output data using WIMS UTILITIES 2.0.3 [9]. Full core, 3D diffusion calculations were performed with RFSP 3.5.1 [10]. RFSP uses, as input, two-group homogenized cross sections, which are produced by homogenizing results of WIMS-AECL calculations with the WIMS-UTILITIES suite of codes.

The adjuster rods were incorporated into the RFSP core model through the use of incremental cross sections calculated with the code DRAGON 306G [11] using the method described in [12]. The incremental cross sections were determined for a previous 78-element SCWR fuel assembly. The use of incremental cross sections based on this previous fuel assembly concept is deemed to be adequate to

determine qualitative trends of core behaviour and may be refined to reflect the current fuel concept in future studies.

## 4. Results and Discussion

### 4.1 Lattice Physics with Burnable Neutron Absorber

The purpose of adding BNA to fresh fuel is to achieve initial reactivity suppression. The best option for reactivity suppression includes an amount of BNA added to the assembly that:

- 1) Adequately suppresses reactivity initially,
- 2) Has minimal effect on achievable exit burnup,
- 3) Has minimal reactivity swing associated with depletion of burnable absorber.

It has been shown that gadolinium possesses the most favorable characteristics of a neutron absorber: namely that it burns out in a time long enough to provide initial reactivity suppression, but not too long as to adversely affect fuel burnup.

Scoping to determine an appropriate concentration of gadolinia to add to the fuel was done through WIMS-AECL lattice calculations. As described in Section 2.1 and illustrated in Figure 1, the gadolinia was added to eight of the fuel elements in each ring of fuel. Shown in Figure 4 are the results of lattice reactivity vs. burnup for three concentrations of gadolinia plus the case where no BNA was added. Based on these results, the concentration of 4% gadolinia in 16 fuel pins was determined to provide adequate reactivity suppression with little decrease in lattice exit burnup. When compared to the case with no BNA in the fuel, the burn-out period for the gadolinia appears to be slightly more than 40 MWd/kg, i.e. the lattice reactivity returns to that of fuel with no BNA.

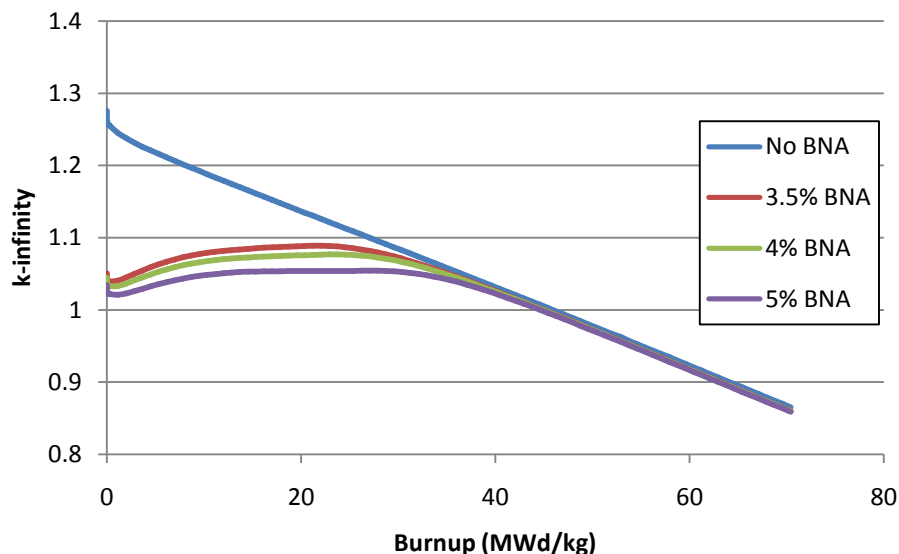


Figure 4 Lattice k-infinity vs burnup for various BNA concentrations

### 4.2 Core Simulations

The SCWR is batch fuelled and has a large excess reactivity at the beginning of each cycle (up to 100 mk when no BNA is present in fresh fuel). Associated with batch fuelling is the need to suppress

the large beginning-of-cycle (BOC) excess reactivity. Further, radial power peaking arising as a consequence of batch refuelling must be mitigated in some way. The core simulations were performed to demonstrate the effectiveness of burnable poisons and adjuster rods and calculate the size of the associated reactivity penalty.

Full core simulations were performed for three cases:

- Full core with neither BNA in the fuel nor adjuster rods.
- Full core with fuel containing BNA, but with no adjuster rods (unrodded).
- Full core with fuel containing BNA and with adjuster rods (rodded).

Results for the core without BNA in the fuel or adjuster rods are shown for comparison with previous results, which also did not include reactivity suppression. Results for the core containing fuel with BNA in the fuel but without adjuster rods are shown in order to better show the impact of the adjuster rods on power shaping. Results for the integral full core performance parameters are shown in Table 3.

**Table 3 Full Core Performance Parameters**

| Parameter                                 | Core with no BNA added to Fuel | Reference Core (Unrodded) | Reference Core (Rodded) |
|---|--------------------------------|---------------------------|-------------------------|
| Average initial wt% PuO <sub>2</sub>      | 13.0                           | 13.0                      | 13.0                    |
| Average initial fissile wt% heavy element | 8.6                            | 8.6                       | 8.6                     |
| Average Exit Burnup (MWd/kg)              | 57.5                           | 41.6                      | 41.6                    |
| Cycle Length (EFPD)                       | 405                            | 289.5                     | 289.5                   |
| Excess Reactivity BOC / EOC (mk)          | 100 / 11.8                     | 31.3 / 10.0               | 14.7 / 0.7              |
| Channel Power Peaking Factor BOC / EOC    | 1.30 / 1.21                    | 2.03 / 1.28               | 1.15 / 1.19             |
| Axial Power Peaking Factor BOC / EOC      | 1.20 / 1.05                    | 1.28 / 1.20               | 1.21 / 1.30             |

The results show the reactivity suppression possible through the use of BNA in the fuel and adjuster rod use. A reduction of almost 70 mk is achieved through the use of BNA in fresh fuel. This could not be achieved through soluble poison in the moderator as this would: a) require too much dissolved poison which could lead to precipitation out of solution, b) result in a positive moderator temperature coefficient of reactivity and c) reduce the effectiveness of the reflector.

By using BNA in combination with the adjuster rods, BOC excess reactivity is approximately 15 mk; this is within the realm of possibility for soluble poison in the moderator.

The penalty incurred for using a large amount of neutron absorbing material is substantial. A reduction in the operating cycle of nearly 120 days is observed, corresponding to a reduction in achievable burnup.

#### 4.2.1 Adjuster Rod Positions

The number of adjuster rods and their configuration are based on preliminary scoping analyses, rather than detailed optimization. The results presented here are intended to demonstrate the feasibility of the combined use of BNA and adjuster rods for reactivity suppression and power shaping. Further optimization would likely yield further improvements in the core channel power distribution and reduce the impact on achievable exit burnup.

The positions of the adjuster rods are shown in Figure 5. The side view of the reactor is shown in Figure 5B, showing the five banks of seven horizontal rods. On the opposite side of the reactor are another five banks of seven rods, making a total of 14 rods that can be moved independently. The top view, showing all rods inserted is in Figure 5A. A side view, showing the axial positions of the adjuster rods, is given in Figure 5B.

These rods are expected to sit in the core during normal operation and are moved as necessary to provide flux shaping. Figure 5C and D show rod positions at beginning (BOC) and end of cycle (EOC), respectively.

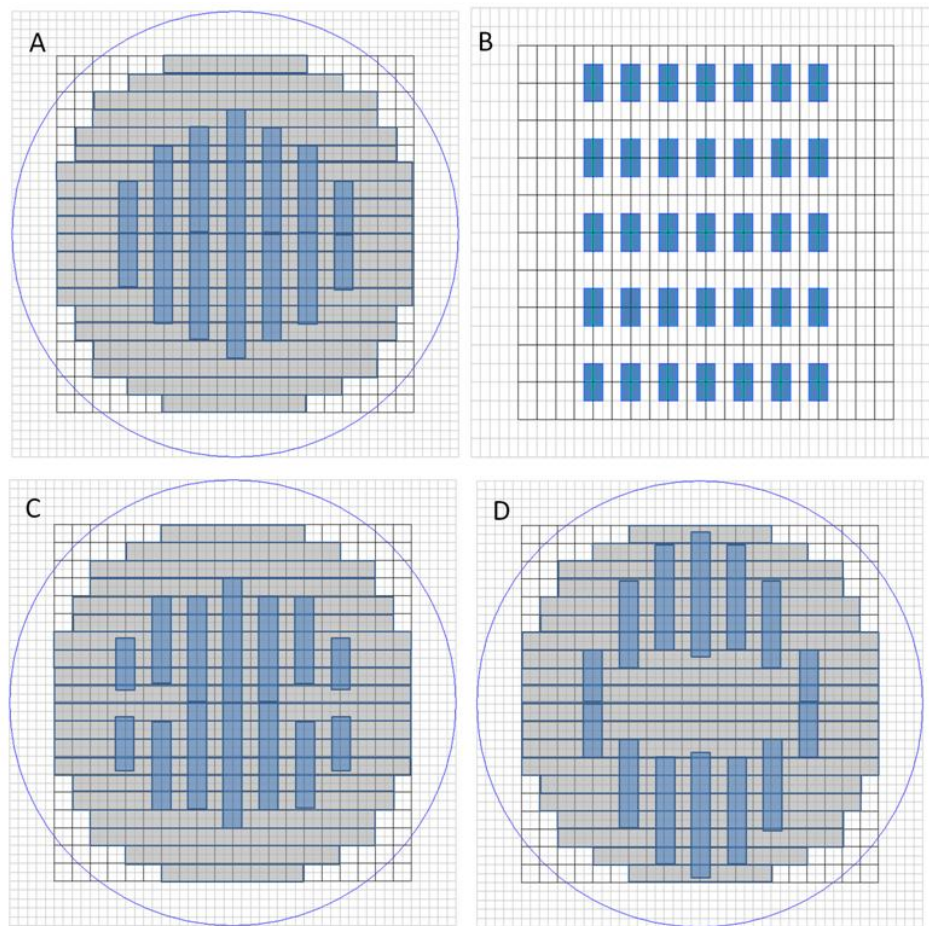


**Figure 5 Cross-sectional view of the full core channel layout, showing positions of inserted horizontal reactivity devices. A) Top view adjuster rod reference positions. B) Side view showing five banks of rods. C) Middle bank of rods at BOC position. D) Middle bank of rods at EOC positions**

### 4.3 Core Power Profiles

#### 4.3.1 Reference Core: No BNA No Adjuster Rods

The beginning and end of cycle radial power profiles are shown in Figure 6 respectively for the core using no BNA in fresh fuel. The channel powers shown in the figures are normalized to the average channel power of the reactor (2540 MW/336 channels = 7560 kW).

The axial power profiles for the highest power channel at BOC and EOC are shown in Figure 7.

|   | 1    | 2    | 3    | 4    | 5    | 6    | 7    | 8    | 9    | 10   |     |
|---|------|------|------|------|------|------|------|------|------|------|-----|
| A |      |      |      |      |      |      | 0.85 | 0.97 | 0.79 | 1.07 | BOC |
|   |      |      |      |      |      |      | 0.93 | 1.04 | 0.84 | 1.10 | EOC |
| B |      |      |      |      | 0.95 | 0.90 | 1.02 | 0.82 | 1.06 | 0.85 |     |
|   |      |      |      |      | 1.05 | 0.99 | 1.10 | 0.87 | 1.10 | 0.88 |     |
| C |      |      | 0.73 | 0.65 | 0.71 | 1.06 | 0.86 | 1.12 | 0.89 | 1.18 |     |
|   |      |      | 0.87 | 0.76 | 0.80 | 1.13 | 0.90 | 1.14 | 0.90 | 1.18 |     |
| D |      |      | 0.65 | 0.92 | 0.92 | 1.03 | 1.03 | 0.92 | 0.99 | 1.02 |     |
|   |      |      | 0.76 | 1.04 | 1.00 | 1.05 | 1.03 | 0.92 | 1.00 | 1.02 |     |
| E |      | 0.95 | 0.71 | 0.92 | 0.92 | 1.28 | 1.12 | 1.24 | 1.03 | 0.88 |     |
|   |      | 1.05 | 0.80 | 1.00 | 0.93 | 1.21 | 1.06 | 1.17 | 1.00 | 0.86 |     |
| F |      | 0.90 | 1.06 | 1.03 | 1.28 | 1.04 | 1.30 | 0.95 | 0.91 | 1.22 |     |
|   |      | 0.99 | 1.13 | 1.05 | 1.21 | 0.96 | 1.18 | 0.88 | 0.85 | 1.13 |     |
| G | 0.85 | 1.02 | 0.86 | 1.03 | 1.12 | 1.30 | 0.98 | 1.07 | 1.25 | 0.96 |     |
|   | 0.93 | 1.10 | 0.90 | 1.03 | 1.06 | 1.18 | 0.90 | 0.99 | 1.14 | 0.89 |     |
| H | 0.97 | 0.82 | 1.12 | 0.92 | 1.24 | 0.95 | 1.07 | 1.14 | 1.10 | 1.08 |     |
|   | 1.04 | 0.87 | 1.14 | 0.92 | 1.17 | 0.88 | 0.99 | 1.05 | 1.02 | 1.01 |     |
| J | 0.79 | 1.06 | 0.89 | 0.99 | 1.03 | 0.91 | 1.25 | 1.10 | 0.96 | 1.08 |     |
|   | 0.84 | 1.10 | 0.90 | 1.00 | 1.00 | 0.85 | 1.14 | 1.02 | 0.90 | 1.01 |     |
| K | 1.07 | 0.85 | 1.18 | 1.02 | 0.88 | 1.22 | 0.96 | 1.08 | 1.08 | 1.10 |     |
|   | 1.10 | 0.88 | 1.18 | 1.02 | 0.86 | 1.13 | 0.89 | 1.01 | 1.01 | 1.04 |     |

Figure 6 BOC and EOC Normalized Channel Powers (No BNA, No Rods)

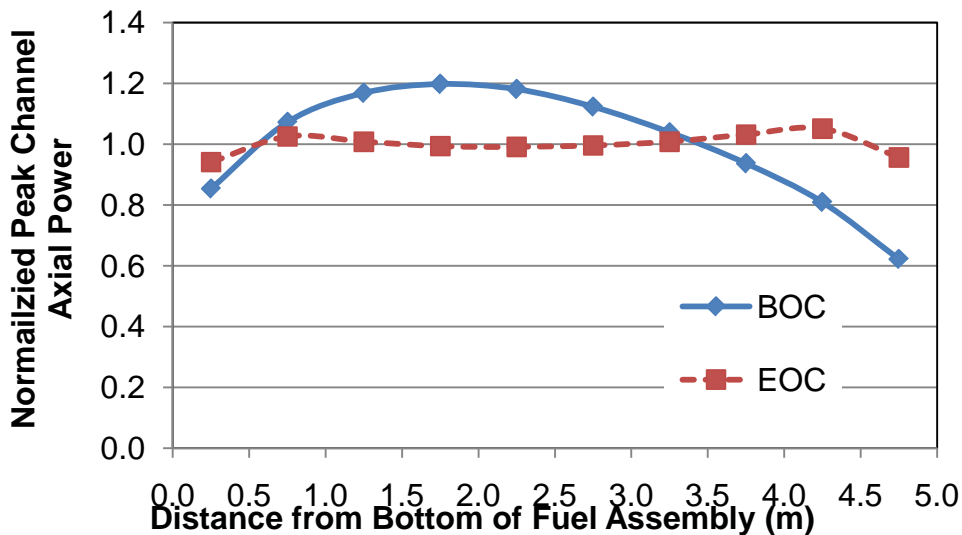


Figure 7 Axial Channel Power Profile (No BNA, No Rods)

4.3.2 Core With BNA and No Adjuster Rods

Core power profiles for BOC and EOC for the unrodded core are shown in Figure 8 while Figure 9 shows the high power channel axial power profile at BOC and EOC. Compared to the core with no BNA added to the fuel, the power is more sharply peaked in the centre of the core. This effect is due to the burn-out period of the gadolinia in the fuel.

|   | 1    | 2    | 3    | 4    | 5    | 6    | 7    | 8    | 9    | 10   |     |
|---|------|------|------|------|------|------|------|------|------|------|-----|
| A |      |      |      |      |      |      | 0.55 | 0.52 | 0.54 | 0.57 | BOC |
|   |      |      |      |      |      |      | 0.78 | 0.77 | 0.71 | 0.82 | EOC |
| B |      |      |      |      | 0.51 | 0.60 | 0.61 | 0.61 | 0.68 | 0.69 |     |
|   |      |      |      |      | 0.79 | 0.88 | 0.87 | 0.77 | 0.91 | 0.84 |     |
| C |      |      | 0.40 | 0.48 | 0.55 | 0.69 | 0.76 | 0.83 | 0.89 | 0.89 |     |
|   |      |      | 0.61 | 0.67 | 0.74 | 0.97 | 0.90 | 1.04 | 0.99 | 1.09 |     |
| D |      |      | 0.48 | 0.59 | 0.74 | 0.86 | 0.97 | 1.03 | 1.09 | 1.10 |     |
|   |      |      | 0.67 | 0.85 | 0.99 | 1.10 | 1.09 | 1.06 | 1.10 | 1.12 |     |
| E |      | 0.51 | 0.55 | 0.74 | 0.79 | 0.96 | 1.10 | 1.13 | 1.21 | 1.14 |     |
|   |      | 0.79 | 0.74 | 0.99 | 0.93 | 1.18 | 1.15 | 1.18 | 1.13 | 0.96 |     |
| F |      | 0.60 | 0.69 | 0.86 | 0.96 | 1.09 | 1.19 | 1.21 | 1.24 | 1.31 |     |
|   |      | 0.88 | 0.97 | 1.10 | 1.18 | 1.10 | 1.21 | 0.99 | 0.96 | 1.14 |     |
| G | 0.55 | 0.61 | 0.76 | 0.97 | 1.10 | 1.19 | 1.34 | 1.47 | 1.48 | 1.50 |     |
|   | 0.78 | 0.87 | 0.90 | 1.09 | 1.15 | 1.21 | 1.09 | 1.15 | 1.21 | 1.02 |     |
| H | 0.52 | 0.61 | 0.83 | 1.03 | 1.13 | 1.21 | 1.47 | 1.62 | 1.73 | 1.78 |     |
|   | 0.77 | 0.77 | 1.04 | 1.06 | 1.18 | 0.99 | 1.15 | 1.24 | 1.22 | 1.21 |     |
| J | 0.54 | 0.68 | 0.89 | 1.09 | 1.21 | 1.24 | 1.48 | 1.73 | 1.79 | 1.95 |     |
|   | 0.71 | 0.91 | 0.99 | 1.10 | 1.13 | 0.96 | 1.21 | 1.22 | 1.06 | 1.23 |     |
| K | 0.57 | 0.69 | 0.89 | 1.10 | 1.14 | 1.31 | 1.50 | 1.78 | 1.95 | 2.03 |     |
|   | 0.82 | 0.84 | 1.09 | 1.12 | 0.96 | 1.14 | 1.02 | 1.21 | 1.23 | 1.25 |     |

Figure 8 BOC and EOC Normalized Channel Powers (With BNA, No Rods)

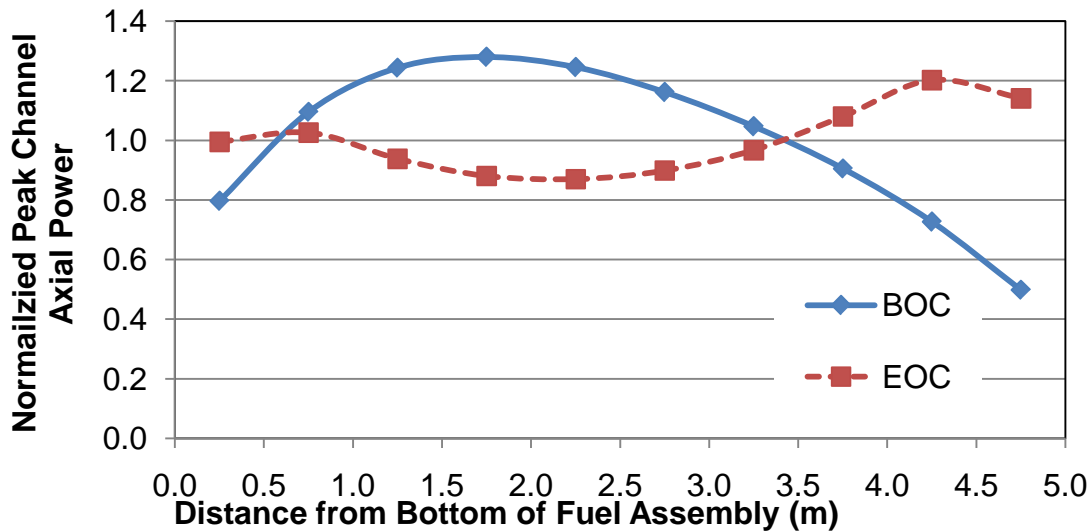


Figure 9 Axial Channel Power Profiles (with BNA, no Rods)

4.3.3 Core With BNA and With Adjuster Rods

Power profiles for BOC and EOC for the rodded core with BNA are shown in Figure 10 while the axial power profiles for the high power channel at BOC and EOC are shown in Figure 11. The adjuster rods were changed at 50 day intervals in the simulation in an attempt to flatten the radial power distribution. The coarse adjuster rod movements used in the simulation were able to maintain a maximum channel power peaking factor of less than 1.2. It should be noted that the adjuster movements in this simulation do not represent optimal rod positions. The results shown here should be interpreted as demonstrating that power shaping is possible using the adjuster rods. It is anticipated that further refinement of the rod movement scheme, in combination with a revised refuelling scheme will lower the radial power peaking factor further.

|   | 1    | 2    | 3    | 4    | 5    | 6    | 7    | 8    | 9    | 10   |     |
|---|------|------|------|------|------|------|------|------|------|------|-----|
| A |      |      |      |      |      |      | 0.87 | 0.82 | 0.86 | 0.84 | BOC |
|   |      |      |      |      |      |      | 0.95 | 0.90 | 0.83 | 0.88 | EOC |
| B |      |      |      | 0.86 | 0.95 | 0.92 | 0.93 | 0.94 | 0.93 |      |     |
|   |      |      |      | 0.99 | 1.03 | 1.01 | 0.87 | 0.92 | 0.81 |      |     |
| C |      |      | 0.72 | 0.88 | 0.94 | 1.01 | 1.06 | 1.05 | 1.02 | 1.02 |     |
|   |      |      | 0.82 | 0.88 | 0.92 | 1.10 | 0.99 | 0.99 | 0.84 | 0.96 |     |
| D |      |      | 0.89 | 0.97 | 1.10 | 1.13 | 1.14 | 1.06 | 1.10 | 1.00 |     |
|   |      |      | 0.89 | 1.06 | 1.11 | 1.14 | 1.11 | 0.88 | 0.92 | 0.87 |     |
| E |      | 0.87 | 0.95 | 1.11 | 1.12 | 1.04 | 1.04 | 0.98 | 0.99 | 0.92 |     |
|   |      | 1.04 | 0.95 | 1.13 | 1.07 | 1.17 | 1.09 | 0.96 | 0.86 | 0.77 |     |
| F |      | 0.97 | 1.03 | 1.15 | 1.11 | 0.96 | 0.95 | 0.93 | 0.90 | 0.90 |     |
|   |      | 1.10 | 1.17 | 1.17 | 1.18 | 0.93 | 0.99 | 0.84 | 0.79 | 0.86 |     |
| G | 0.90 | 0.95 | 1.07 | 1.11 | 1.08 | 0.97 | 0.94 | 0.98 | 0.94 | 0.92 |     |
|   | 1.05 | 1.11 | 1.07 | 1.14 | 1.11 | 1.01 | 0.86 | 0.92 | 0.94 | 0.82 |     |
| H | 0.86 | 0.97 | 1.07 | 1.00 | 1.01 | 0.98 | 1.01 | 1.03 | 1.03 | 1.03 |     |
|   | 1.03 | 1.00 | 1.16 | 0.94 | 1.03 | 0.89 | 0.95 | 1.02 | 1.02 | 1.01 |     |
| J | 0.91 | 1.00 | 1.08 | 1.08 | 1.07 | 1.01 | 1.03 | 1.07 | 1.07 | 1.09 |     |
|   | 0.96 | 1.10 | 1.01 | 1.05 | 0.99 | 0.89 | 1.04 | 1.09 | 1.05 | 1.09 |     |
| K | 0.90 | 1.01 | 1.11 | 1.15 | 1.12 | 1.12 | 1.12 | 1.10 | 1.11 | 1.12 |     |
|   | 1.06 | 1.00 | 1.18 | 1.07 | 0.95 | 1.01 | 0.93 | 1.14 | 1.18 | 1.14 |     |

Figure 10 BOC and EOC Normalized Channel Powers (with BNA, with Rods)

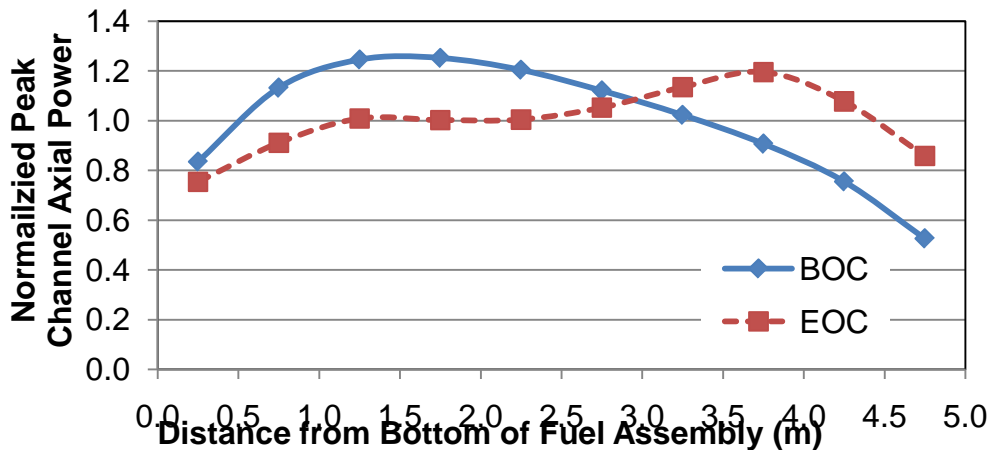


Figure 11 Axial Channel Power Profile (with BNA, with Rods)

## 5. Summary and Conclusions

The use of BNA in SCWR fuel assemblies and adjuster rods for reactivity suppression and power shaping were examined. It has been demonstrated that the combination of BNA in the fuel and adjuster rods in the core can be successfully applied to suppress excess reactivity during operation and to improve (flatten) the channel power distribution. The use of BNA and adjuster rods, however, does result in a significant penalty to the maximum achievable exit burnup. Further optimization of the use of BNA and adjuster rods may lead to improvements in maximum achievable exit burnup and in the channel power distribution.

## 6. References

- [1] K. Boyle, D. Brady, D. Guzonas, H. Khartabil, L. Leung, J. Lo, S. Quinn, S. Suppiah, and W. Zheng, “Canada’s Generation-IV National Program – Overview”, 4th International Symposium on Supercritical Water-Cooled Reactors, Heidelberg, Germany, March 8-11, 2009.
- [2] J. Pencer, A. Colton, X. Wang, M. Gaudet, H. Hamilton, and M. Yetisir, “Evolution of the Core Physics Concept for the Canadian Supercritical Water Reactor”, Global 2013, Salt Lake City, Utah, September 29-October 3, 2013.
- [3] J. Pencer and A. Colton, “Progression of the Lattice Physics Concept for the Canadian Supercritical Water Reactor”, Proceedings of the 34th Annual Conference of the Canadian Nuclear Society, June 09-12, 2013.
- [4] J. Pencer, D. Watts, A. Colton, X. Wang, L. Blomeley, V. Anghel, and S. Yue, “Core Neutronics for the Canadian SCWR Conceptual Design”, The 6th International Symposium on Supercritical Water-Cooled Reactors, ISSCWR-6, Shenzhen, Guangdong, China, March 03- 07, 2013.
- [5] J. Pencer, M. McDonald, V. Anghel, “Parameters for Transient Response Modeling for the Canadian SCWR”, The 19th Pacific Basin Nuclear Conference – PBNC 2014, Vancouver, BC, August 24-28, 2014.
- [6] M. Yetisir, M. Gaudet, J. Bailey, D. Rhodes, D. Guzonas, H. Hamilton, Z. Haque, J. Pencer, A. Sartipi, “Reactor Core and Plant Design Concepts of the Canadian Supercritical Water-Cooled Reactor”, 2014 Canada-China Conference on Advanced Reactor Development, Niagara Falls, Ontario, April 27-30, 2014.
- [7] D.V. Altiparmakov, “New Capabilities of the Lattice Code WIMS-AECL”, Proc of. PHYSOR 2008: International Conference on Reactor Physics, Nuclear Power: A Sustainable Resource, Casino-Kursaal Conference Center, Interlaken, Switzerland, September 14-19, 2008.
- [8] D.V. Altiparmakov, “ENDF/B-VII.0 Versus ENDF/B-VI.8 in CANDU Calculations”, Proc. Of PHYSOR 2010: Advances in Reactor Physics to Power the Nuclear Renaissance, Pittsburgh, Pennsylvania, USA, May 9-14, 2010.
- [9] T. Liang, W. Shen, E. Varin and K. Ho, “Improvement and Qualification of WIMS UTILITIES”, 29th Annual Conference of the Canadian Nuclear Society, Marriott Eaton Centre, Toronto, Ontario, June 1-4, 2008.

- [10] B. Rouben, “RFSP-IST, the Industry Standard Tool Computer Program for CANDU Reactor Core Design and Analysis”, Proc. of the 13th Pacific Basin Nuclear Conference (PNBC-2002), Shenzhen, China, 2002.
- [11] G. Marleau, A. Hébert and R. Roy, “A User Guide for DRAGON. Version DRAGON\_000331 Release 3.04”, Report IGE-174 Rev. 5, Institut de génie nucléaire, École Polytechnique de Montréal, Montréal, Québec, 2000.
- [12] R. S. Davis, “Qualification of DRAGON for Reactivity Device Calculation in the Industry Standard Toolset,” Proceedings of the 25th Annual CNS Conference, Toronto, Ontario, Canada, June 6-9, 2004.